Radio Emission Associated with Ultraluminous X-ray Sources in the Galaxy Merger NGC 3256

S. G. Neff
Laboratory for Astronomy and Solar Physics, NASA's Goddard Space Flight Center, Greenbelt, MD 20771
susan.g.neff@nasa.gov

James S. Ulvestad
National Radio Astronomy Observatory, P. O. Box 0, Socorro, NM 87801
julvesta@aoc.nrao.edu
and

S. D. Campion
SSAI and GSFC
scampion@hst.nasa.gov

ABSTRACT

We present new 6, 3.6, and 2 cm VLA radio observations of the nearby merger system NGC 3256, with resolutions of $\sim$ 100 pc, which reveal compact radio sources embedded in more diffuse emission at all three wavelengths. The two radio nuclei are partially resolved, but the two dominant compact sources that remain coincide with the two most powerful compact Ultraluminous X-ray sources (ULXs) recently reported by Lira *et al.* The radio/X-ray ratios for these two sources are too high by factors of >100–1000 to be normal X-ray binaries. However, their radio and X-ray powers and ratios are consistent with low-luminosity active galactic nuclei (LLAGNs), and optical emission lines suggest the presence of a nuclear disk around the northern nucleus. If the two nuclear ULXs are LLAGNs, their associated black holes are separated by only $\sim$1kpc, about 6 times closer to one another than those found recently in the merger galaxy NGC 6240. A third ULX on the outskirts of the merger is also a radio source, and probably is a collection of supernova remnants. The remaining ULXs are not coincident with any source of compact radio emission, and are consistent with expectations for beamed X-ray binaries or intermediate-mass black holes.

Subject headings: galaxies: individual (NGC 3256) — galaxies: interactions — galaxies: starburst — galaxies: star clusters — X-rays: binaries — X-rays: galaxies

1. Introduction

NGC 3256 is a well-studied merging galaxy system and is the brightest IR source in the nearby universe, with a luminosity of $3 \times 10^{11} L_{\odot}$ in the 8–1000 μm range (Sargent, Sanders, & Phillips 1989), after conversion to a distance of 37 Mpc (H_0 = 75 km s^{-1} Mpc^{-1}). It is also at the top end of the X-ray luminosity range for starburst galaxies (Lira et al. 2002). Tidal tails extending $\sim$ 200 kpc and other morphological and kinematical evidence (deVaucouleurs & deVaucouleurs 1961; Toomre 1977; Feast & Robertson 1978; Schweizer 1986) suggest that the system was composed of two gas-rich disks, which coalesced $\sim$1 galaxy crossing time ago (Keel & Wu 1995). However, two "nu-

clei" are detected at radio and NIR wavelengths, suggesting that the progenitors may not have completed their merger (Norris & Forbes 1995; Kotilainen et al. 1996). All observations to date suggest that the system properties are best explained by an ongoing very intense starburst and associated superwind (Lipari et al. 2000).

Recently, high-resolution *Chandra* observations of NGC 3256 detected 14 discrete hard X-ray sources with luminosities of 10^{39}–$10^{40.5}$ ergs s^{-1} at an assumed distance of 56 Mpc (Lira et al. 2002); 13 of these remain above 10^{39} ergs s^{-1} for a distance of 37 Mpc. Such sources are referred to as Ultraluminous X-ray sources (ULXs), since their isotropic luminosities are far above the Eddington limit of 2×10^{38} ergs s^{-1} for an accreting $1.4M_{\odot}$ neutron star in an X-ray binary, but below the limit for classical active galactic nuclei (AGNs), $\sim 10^{42}$ ergs s^{-1}. Possible explanations for ULXs include accreting intermediate-mass ($\sim$100–1000 M$_{\odot}$) black holes (IMBH; probably in binaries), beamed "normal" X-ray binaries, microquasars, transient super-Eddington accretors, young supernova remnants (SNRs) in extremely dense environments, hypernovae/GRB's, or background BL Lac objects (Fabbiano 1989; Marston et al. 1995; Colbert & Mushotzky 1999; Makishima et al. 2000; King et al. 2001; King 2002; Roberts et al. 2003). The first large samples of ULXs suggested that they are fairly rare in normal galaxies (Roberts & Warwick 2000), but much more common, and brighter, in merging and starburst galaxies (Fabbiano, Zezas, & Murray 2001; Kaaret et al. 2001). Efforts to identify ULX counterparts at other wavelengths have had limited success: a ULX in NGC 5204 may be associated with a young optical star cluster (Roberts et al. 2001; Goad et al. 2002), at least four ULXs are associated with X-ray ionized nebulae or SNR (Pakull & Mironi 2002; Roberts et al. 2003), several ULXs in elliptical galaxies may be in globular clusters (Wu et al. 2002; Angelini et al. 2001), and a radio counterpart recently has been identified for a ULX in NGC 5408 (Kaaret et al. 2003).

Centimetric radio observations penetrate the dust causing the optical obscuration in starbursts. If radio emission is associated with a ULX, the radio luminosity and spectrum can be used to constrain possibilities for the ULX identity. Previous radio imaging of NGC 3256 identified two bright steep-spectrum nuclear sources (Norris & Forbes 1995), but had insufficient resolution to probe the ULX environment. Here, we present new, high-resolution radio images of NGC 3256 that provide new clues to the nature of its ULXs.

2. Radio Images and Measurements

NGC 3256 was observed in 2001 February (**BnA** configuration) and 2002 April (**A** configuration) using the NRAO[1] Very Large Array (VLA) at 6 cm (4860 MHz) and 3.6 cm (8460 MHz), for $\sim$ 7.5hrs each. A 12-minute 2 cm (14940 MHz) observation was obtained in 2002 April, and a 35-minute 2 cm observation at lower resolution (**CnB** configuration) from 1986 was retrieved from the VLA archive. The data were calibrated, self-calibrated, and imaged as described in Neff & Ulvestad (2000). Typical resolutions (FWHM) are 50-60 pc ($\sim$0.″35) by 140–180 pc (0.″7–1.″0).

We measured flux densities of compact radio sources associated with ULXs by fitting a parabola to the peak, and derived the amount of diffuse emission around the selected sources by integrating over a specified box and subtracting the flux of the related compact source (Table 1). Errors in radio positions are $\lesssim$0.″1, negligible compared to the X-ray position uncertainties[2] of $\gtrsim$0.″6; radio flux densities have typical (1σ) errors of 5% at 3.6 and 6 cm, and 10% at 2 cm.

At both 6 cm and 3.6 cm, two bright compact sources are embedded in diffuse extended emission (Figure 1). No radio emission is detected outside the central 40″ (7 kpc) of the galaxy, with respective 3σ limits of $\sim$36 and $\sim$30 μJy beam^{-1} at 6 and 3.6 cm. At the highest resolution (Figure 2, **A** configuration only), 3.6 and 2 cm images resolve both of the bright nuclear sources into several discrete components. ULX positions from Lira et al. (2002) are indicated on each image (Figures 1 and 2), with the Lira et al. (2002) source numbers used in the remainder of this paper.

[1]The National Radio Astronomy Observatory is a facility of the National Science Foundation operated under cooperative agreement by Associated Universities, Inc.

[2]see the *Chandra* Proposer's Guide v 4.0, 2001, http://asc.harvard.edu/udocs/docs/POG/MPOG

3. Identification of Radio Sources Associated with ULXs

ULXs 7 and 8 are coincident with compact radio sources, and ULX 13 is at the location of an extended, partly resolved radio source. Properties of these radio sources are given in Table 1. Radio emission is found at the edges of the 1.″8 radius (3σ) *Chandra* error circles of several other ULXs in NGC 3256, but is neither compact nor precisely coincident with the X-ray position (see Fig. 1): for example, ULXs 9, 10, and 11 are clustered around the edges of a group of compact radio sources, ULX 2 is near the edge of another, as shown in Figure 1. Lira et al. (2002) note that these are sites of massive stars ionizing their surroundings, as evidenced by strong Hα emission (Lipari et al. 2000). The nominal separations of $\sim 2''$ between radio emission and ULXs correspond to ~ 360 pc in NGC 3256.

Figure 2 shows that ULXs 7 and 8 nominally coincide with the two most compact nuclear radio peaks. Lira et al. (2002) indicate that the northern X-ray source, ULX 7, is resolved, with a size of $\sim 1''$–$1.''5$ ($\sim$180–270 pc); they suggest that this corresponds to "a compact grouping of individual sources ... at the heart of the nuclear starburst." However, Mushotzsky (priv. comm) has determined that ULX 7 is a dominant point source (unresolved by *Chandra*) embedded in low-level extended emission, as can be seen in Fig 2c. Our 3.6 and 2 cm images (Fig. 2a,b) indicate that the radio emission at this position is partially resolved on a similar scale and is also embedded in extended emission.

4. Nature of the Ultraluminous X-ray Sources

The radio sources near ULXs 7 and 8 have respective spectral indices of $\alpha = -1.04$ and $\alpha = -0.74$ (for $S_\nu \propto \nu^\alpha$) between 3.6 and 2 cm, indicative of optically thin synchrotron emission. However, the source spectra flatten between 6 and 3.6 cm in matched-resolution images ($\alpha = -0.49$ and $\alpha = -0.16$), which may indicate that some of the subcomponents are free-free absorbed at longer wavelengths. For gas at 6000 K (Lipari et al. 2000), the required emission measure for significant free-free absorption at 5 GHz is about 5×10^7 cm^{-6} pc. This implies (for example) a typical ionized density of ~ 7000 cm^{-3} for a path length of ~ 1 pc, or ~ 700 cm^{-3} for a path length of 100 pc. The density in the latter case is similar to that found by Lipari et al. (2000) on scales of a few hundred parsecs, but the relatively low filling factor of the gas seen on these large scales makes it likely that any free-free absorption would be caused by higher density gas on scales of a parsec or less.

We use the ratio of 6-cm radio emission to 2–10 keV X-ray emission, $R_X \equiv L_R/L_X = \nu L_\nu(5\ \mathrm{GHz})/L_X(2{-}10\,\mathrm{keV})$, defined by Terashima & Wilson (2003), to distinguish further among possible origins of ULXs 7 and 8. Table 2 gives values of this ratio for ULXs in NGC 3256 and for a number of comparison objects. First, consider flaring X-ray transients. ULXs 7 and 8 might be either beamed "normal" binaries or unbeamed binaries including intermediate-mass black holes ($\sim$ 100–1000$M_\odot$). Using the peak values in both wavebands, Fender & Kuulkers (2001) compile values of the radio/X-ray ratio for galactic X-ray transients in outburst, and show that it always is less than 10^4 mJy Crab^{-1}, corresponding to $R_X < 2.3 \times 10^{-5}$. This is consistent with the result of Kaaret et al. (2003), who interpret a ULX in NGC 5408 as a beamed X-ray transient (although they note it could also be an IMBH); the faint radio detection implies $R_X < 10^{-5}$. In contrast, ULXs 7 and 8 in NGC 3256 have R_X well above 10^{-3}, much larger than the ratio for galactic X-ray transients; the radio flux densities are more than 10^5 times stronger than expected from Cygnus X-1 beamed toward us from a distance of 37 Mpc (Georganopoulos, Aharonian, & Kirk 2002).

The northern nucleus of NGC 3256 (ULX 7) is known to harbor an extreme starburst (Lipari et al. 2000), so it is worth considering whether the radio and X-ray emission can be produced by only young stars or associated high mass X-ray binaries (HMXB) Optical and UV emission lines suggest that the ensemble of stars in the northern nucleus has $T_{\rm eff} = 35,000$ K (Lipari et al. 2000), and the X-ray spectrum is consistent with a hot-gas component at $\sim 2 \times 10^7$K (Lira et al. 2002). A strong upper limit to the number of stars present can be calculated by assuming that the entire 3 mJy flux density at 2 cm is due to thermal emission from ionized gas (unlikely due to the steep ra-

dio spectrum); this would require the equivalent of $\sim 10^5$ O7 stars (Vacca 1994). These hot stars would generate X-ray emission primarily in stellar winds; the expected X-ray luminosity from 10^5 O7 stars would be $\sim 10^{37}$ ergs s^{-1} (Long & White 1980; Chlebowski, Harnden, & Sciortino 1989), a factor of 1000 below the observed X-ray luminosity. It is likely that a cluster of O stars will contain a significant number of HMXB's. If systems like Cyg X-1 (Georganopoulos, Aharonian, & Kirk 2002) were to produce all of the ULX 7 X-ray emission, ∼600-1000 such systems would be required, 1 per 100 O stars. These HMXBs would produce $< 10^{-4}$ of the observed radio emission. Although it is possible that the radio and X-ray emission could come from a combination of O stars and many HMXBs, it seems unlikely that this many HMXB's would have already formed while there are still $\sim 10^5$ unevolved O stars.

Since the X-ray and radio sources in ULX 7 both contain multiple components (diffuse and discrete), it seems useful to compare R_X for ULX 7 with better-resolved starburst region in a nearby galaxy. NGC 253, at a distance of ~ 2.6 Mpc, has an X-ray flux of $\sim 2.5 \times 10^{-12}$ ergs s^{-1} (Weaver et al. 2002) in its central 5″ (60 pc); integrating over the same area in the 5 GHz VLA image from Antonucci & Ulvestad (1988) yields a flux density of ~ 600 mJy. For this compact nuclear starburst, therefore, $R_X \sim 1 \times 10^{-2}$, a factor of only a few higher than ULX 7. This suggests that ULX 7 may represent a region of extreme "nuclear" star formation.

Next, we consider the possibility that ULXs 7 and 8 produce X-ray and radio emission in multiple SNRs. For the galactic SNR Cas A, $L_R/L_X \approx 0.02$, similar to the values for ULXs 7 and 8 (Cas-A X-ray flux from http://hea-www.harvard.edu/ChandraSNR /G111.7-02.1/; contemporaneous radio flux density derived from Baars et al. 1977). The total radio and X-ray fluxes are ~ 1000 times stronger than Cas A would be at 37 Mpc, implying that many similar SNRs would be required within a volume of 10^5–10^6 pc^3. In the case of ULX 13, associated with a partially resolved steep-spectrum radio source well away from the galaxy nuclei, $R_X \sim 0.01$, also consistent with Cas A, with total emission ~ 200 times more powerful. Some young radio supernovae may have radio powers of tens to hundreds times that of Cas A (Weiler et al. 1986), but accounting for the relatively steady radio emission from the NGC 3256 nuclei still would require many supernovae over at least the last 15 yr. The same arguments apply to the case of hypernovae (Roberts et al. 2003), with the additional constraint that NGC 3256 has not been identified with any GRB's.

A final possibility is that ULXs 7 and 8 are low-luminosity AGNs (LLAGNs), generated in or fueled by the galaxy merger. Lira et al. (2002) note that the X-ray properties and overall SED of ULX 8 are consistent with this possibility, but suggest that ULX 7 is to be too strong at 10μm to be an AGN. However, Ho (1999) shows that LLAGNs have a maximum in the SED at ∼10μm. Ho (1999) also finds, when different classes of AGN SEDs are normalized at 1 keV, that LLAGNs are considerably stronger at mid-IR wavelengths than other classes of AGN (Lira et al. (2002) made the SED comparison by normalizing various AGN SEDs at 3.5μm). Thus, Ho (1999)'s work stongly supports the idea that ULX 7 is also a LLAGN. Both ULXs 7 and 8 have values of R_X well within the range for radio-loud AGNs, defined by Terashima & Wilson (2003). R_X for ULXs 7 and 8 is a factor of a few larger than for several LLAGNs at comparable distances (Ulvestad & Ho 2001) and for the nearby galaxy nucleus in M32 (Ho, Terashima, & Ulvestad 2003), and is similar to the values for the two AGNs in the merger NGC 6240 (Komossa et al. 2003). Further evidence for the LLAGN possibility comes from examination of archival HST long-slit spectra of the northern nucleus, which show broadened Hα, Hβ, [N II], and [S II] emission lines with linewidths of ∼450 km sec^{-1}, as shown in Figure 3. The emission line show a rotation-curve-like shear in their peak velocities of ∼300km sec^{-1} over a projected distance of ∼40pc. If we assume this shear indicates rotation of a nuclear disk, it implies that ULX 7(N) has a mass of *at least* 10^8M$_\odot$ within ~ 40 pc.

LLAGNs are the most plausible explanation for ULXs 7 and 8 in NGC 3256, although large collections of supernova remnants are also consistent with their radio/X-ray ratios and powers. If ULXs 7 and 8 are LLAGN, the dual black holes are separated by only ~ 1 kpc, considerably closer than the ~ 6 kpc separation for the dual AGNs in NGC 6240.

For the remaining ULXs that are not associated

with discrete radio sources, the radio/X-ray limits are consistent with expectations for high-mass X-ray binaries, either beamed or accreting at super-Eddington rates, and ULX 13 is also consistent with a collection of confined SNRs.

5. Summary

We have presented new, high resolution, sensitive radio images of the merging galaxy NGC 3256. We found that three compact radio sources appear to be identified with ULX's. Two of the ULX's are coincident with the two galaxy nuclei, and have properties indicative of being two LLAGN, separated by ~ 6 pc. Radio properties of a third ULX suggest that is is a large complex of supernova remnants, and the remaining ULX's are likely associated with HMXRBs or IMBHs.

Part of this work was supported by NASA grant 344-01-21-77. We thank Vivek Dhawan, Phillip Kaaret, and Richard Mushotzky for useful discussions. SGN and JSU acknowledge the Aspen Center for Physics for hospitality during the preparation of this work. This research has made use of the NASA/IPAC Extragalactic Database (operated by the Jet Propulsion Laboratory, California Institute of Technology, under contract with the National Aeronautics and Space Administration) and of NASA's Astrophysics Data System Bibliographic Services.

REFERENCES

Angelini, L., Loewenstein, M., and Mushotzky, R. F. 2001, ApJ, 557, L35

Antonucci, R. R. J., & Ulvestad, J. S. 1988, ApJ, 330, L97

Baars, J. W. M., Genzel, R., Pauliny-Toth, I. I. K., & Witzel, A. 1977, 1982, A&A, 109, 301

Beswick, R. J., Pedlar, A., Mundell, C. G., & Gallimore, J. F. 2001, MNRAS, 325, 151

Chlebowski, T., Harnden, F. R., Jr., & Sciortino, S. 1989, ApJ, 321, 427

Colbert, E. J. M., & Mushotzky, R. F. 1999, ApJ, 519, 89

deVaucouleurs, G. & deVaucouleurs, A. 1961, MNRAS, 68, 69

Fabbiano, G. 1989, ARA&A, 87, 27.

Fabbiano, G., Zezas, A., & Murray, S. S. 2001, ApJ, 554, 1035

Feast, W. M., & Robertson, B. S. C. 1978, MNRAS, 185, 31

Fender, R. P., & Kuulkers, E. 2001, MNRAS, 324, 923

Georganopoulos, M., Aharonian, F. A., & Kirk, J. G. 2002, A&A, 388, L25

Goad, M. R., Roberts, T. P., Knigge, C., & Lira, P. 2002, MNRAS, 335, L67

Ho, L. C. 1999, ApJ, 516, 672.

Ho, L. C., Terashima, Y., & Ulvestad, J. S. 2003, ApJ, 589, 783

Ho, L. C. 2003, in Active Galactic Nuclei: from Central Engine to Host Galaxy, astro-ph/0303059

Kaaret, P., et al. 2001, MNRAS, 321, L29

Kaaret, P., et al. 2003, Science, 299, 365

Keel, W. C., & Wu, W. 1995, AJ, 110, 129

King, A. R., Davies, M. B., Ward, M. J., Fabbiano, G., & Elvis, M. 2001, ApJ, 552, L109

King, A. R. 2002, MNRAS, 335, L13

Komossa, St., Burwitz, V., Hasinger, G., Predehl, P., Kaastra, J. S., Ikebe, Y. 2003, ApJ, 582, L15

Kotilainen, J. K., Moorwood, A. F. M., Ward, M. J., & Forbes, D. A. 1996, A&A, 305, 107

Lipari, S., Diaz, R., Taniguchi, Y., Terlevich, R., Dottori, H., & Carranza, G. 2000, AJ, 120, 645

Lira, P., Ward, M., Zezas, A., Alonso-Herrero, A., & Ueno, S. 2002, MNRAS, 330, 259

Long, K. S., & White, R. L. 1980, ApJ, 239, L65

Makishima, K., et al. 2000, ApJ, 553, 632

Marston, A. P., Elmegreen, D., Elmegreen, B., Forman, W., Jones, C., & Flanagan, K. 1995, ApJ, 438, 663

Neff, S. G., & Ulvestad, J. S. 2000, AJ, 120, 670

Norris, R. P., & Forbes, D. A. 1995 ApJ, 446, 94

Pakull, M. W. & Mirioni, L. 2002, in New Visions of the Universe in the XMM-Newton and Chandra Era, astro-ph/0202488

Roberts, T. P. & Warwick, R. S. 2000, MNRAS, 315, 98

Roberts, T. P. Goad, M. R., Ward, M. J., Warwick, R. S., O'Brien, P. T., Lira, P., & Hands, A. D. P. 2001, MNRAS, 325, L7

Roberts, T. P., Goad, M. R., Ward, M. J., and Warwick, R. S., 2003, MNRAS, 342, 709 J.,

Sargent, A.I., Sanders. D. B., & Phillips, T. G. 1989, ApJ, 346, L9

Schweizer, F. 1986, Science, 231, 227.

Terashima, Y., & Wilson, A. S. 2003, ApJ, 583, 145

Toomre, A. 1977, in The Evolution of Galaxies and Stellar Populations, ed B. M. Tinsley & R. B. Larson (New Haven, Yale Univ.), 401

Ulvestad, J. S., & Ho, L. C. 2001, ApJ, 562, L133

Vacca, W. D. 1994, ApJ, 421, 140

Weiler, K. W., Sramek, R. A., Panagia, N., van der Hulst, J. M., & Salvati, M. 1986, ApJ, 301, 790

Wu, H., Xue, S. J., Xia, X. Y., Deng, Z. G., Mao, S., 2002, ApJ, 576, 738

Weaver, K. A., Heckman, T. M., Strickland, D. K., & Dahlem, M. 2002, ApJ, 576, L19

Zezas, A., Fabbiano, G., Prestwich, A., Murray, S., & Ward, M. 2001, in The Central kpc of Starbursts and AGN: The La Palma Connection, ASP Conf. Ser. 249, ed. J. H. Knapen, J. E. Beckman, I. Shlosman, & T. J. Mahoney, (San Francisco: ASP), 425

Zezas, A., Georgantopoulos, I, & Ward, M. J., 1998, MNRAS, 301, 915

This 2-column preprint was prepared with the AAS LaTeX macros v5.0.

TABLE 1
DISCRETE RADIO SOURCES AT ULX POSITIONS

ULX	R. A. (J2000)	Decl. (J2000)	S_{6cm} (mJy)	$S_{3.6cm}$ (mJy)	S_{2cm} (mJy)	Resolution (Type)
7(N)	10 27 51.23	-43 54 14.0	$\cdots$	$2.3 \pm .1$	$1.4 \pm .2$	$0\farcs63 \times 0\farcs15$ (peak)
			$5.0 \pm .3$	$3.8 \pm .2$	$2.1 \pm .2$	$1\farcs00 \times 0\farcs26$ (peak)
			31 ± 2	20 ± 1	17 ± 2	$\sim 2\farcs5 \times 3\farcs5$ (box)
8(S)	10 27 51.22	-43 54 19.2	$\cdots$	3.9 ± 0.2	3.0 ± 0.3	$0\farcs63 \times 0\farcs15$ (peak)
			6.0 ± 0.3	5.5 ± 0.3	3.6 ± 0.4	$1\farcs00 \times 0\farcs26$ (peak)
			25 ± 1	16.1 ± 0.8	11 ± 1	$\sim 2\farcs5 \times 3\farcs5$ (box)
13	10 27 52.91	-43 54 11.5	$\cdots$	< 0.08	< 0.24	$0\farcs63 \times 0\farcs15$ (peak)
			0.28 ± 0.03	0.18 ± 0.02	< 0.36	$1\farcs00 \times 0\farcs26$ (peak)
			1.35 ± 0.07	0.88 ± 0.05	0.5 ± 0.2	$\sim 2\farcs5 \times 3\farcs5$ (box)

[a]Peak flux is measured using two different beam sizes (resolution is FWHM) so that spectral indices may be determined for both $\alpha_{3.6}^{6}$ and for $\alpha_{2}^{3.6}$. The smaller beam size is for A-configuration images with restoring beam size (FWHM) $0\farcs63 \times 0\farcs15$, which cannot be obtained at 6 cm. The larger beam size given is the smallest possible at 6 cm. Integrated flux measures, within boxes, are also given; they are used determine diffuse emission spectral indices.

TABLE 2
RADIO/X-RAY PROPERTIES OF ULXS AND COMPARISON OBJECTS

Source	$\alpha_{6-3.6}$	$\alpha_{3.6-2}$	S(5 GHz)[a] (mJy)	$F_{\rm X}$(2–10 keV) (ergs cm^{-2} s^{-1})	R_X[b]	References[c]
ULX 7(N) compact	-0.49	-1.04	5.0	1×10^{-13}	2×10^{-3}	1,2
ULX 8(S) compact	-0.16	-0.74	6.0	3×10^{-14}	1×10^{-2}	1,2
ULX 7(N) diffuse	-0.84	-0.18	26	···	···	1
ULX 8(S) diffuse	-1.01	-0.68	19	···	···	1
ULX 13 diffuse	-0.77	-2.03	1.1	5×10^{-15}	1×10^{-2}	1,2
Other NGC 3256 ULXs	···	···	< 0.05	$\sim 10^{-14}$	$< 2 \times 10^{-3}$	1,2
X-ray transients	···	···	···	···	$< 2 \times 10^{-5}$	3
NGC 5408 ULX	···	···	0.3	3×10^{-12}	5×10^{-6}	4
10^5 O stars at 37 Mpc	~ -0.1	~ -0.1	~ 3	6×10^{-17}	~ 3	1,5,6
Cas A	~ -0.5	~ -0.5	7×10^5	2×10^{-9}	2×10^{-2}	7,8
NGC 253 (nuc)	∼-0.7	...	600	2×10^{-13}	1×10^{-2}	9,10
LLAGNs at 20 Mpc	$\sim +0.3$	$\sim +0.3$	~ 10	$\sim 1 \times 10^{-14}$	$\sim 1 \times 10^{-3}$	11
NGC 6240N	-0.6	-0.6	16	8×10^{-13}	1×10^{-3}	12,13
NGC 6240S	-0.7	-0.7	37	3×10^{-13}	6×10^{-3}	12,13

[a]Compact radio flux densities measured in a beam $1\farcs00 \times 0\farcs26$ (from Table 1).

[b]$R_X = \nu L_\nu(5\ {\rm GHz})/L_X$, as defined by Terashima & Wilson (2003).

[c]References: 1. This paper. 2. Lira et al. (2002). 3. Fender & Kuulkers (2001). 4. Kaaret et al. (2003). 5. Long & White (1980). 6. Chlebowski et al. (1989). 7. Baars et al. (1977). 8. http://hea-www.harvard.edu/ChandraSNR/G111.7-02.1/. 9. Antonucci & Ulvestad (1988) 10. Weaver et al. (2002) 11. Ulvestad & Ho (2001). 12. Beswick et al. (2001). 13. Komossa et al. (2003).

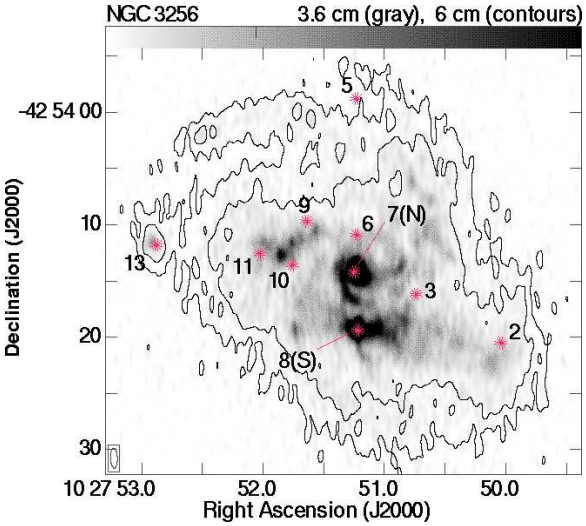

Fig. 1.— 6 cm (contours) and 3.6 cm (grayscale) image of NGC 3256, showing the location of the radio emission relative to the ULX's. Stars show positions of ULXs detected by Lira et al. (2002), with 0.″6 radius indicating the 1σ *Chandra* position uncertainty. The restoring beams are $1.''78 \times 0.''60$ (6 cm) and $1.''01 \times 0.''39$ (3.6 cm), with rms $\sim 13\mu$Jy beam^{-1} and $\sim 9\mu$Jy beam^{-1} respectively. Contours are at 0.07 and 0.15mJy beam^{-1}, gray scale shown ranges from 0.03 to 0.60mJy beam^{-1}, peak flux in 6 cm image is 10.86mJy beam^{-1}, peak flux in 3.6 cm image is 6.18mJy beam^{-1}.

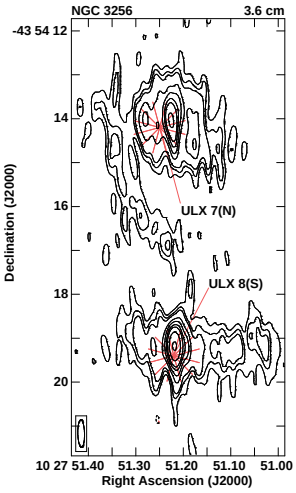

Fig. 2.— 3.6 cm, 2.0cm, and X-ray (1.5-10keV) images of the nuclear region of NGC 3256. Stars mark the positions of ULXs 7 (north nucleus) and 8 (south nucleus) from Lira et al. (2002), with the 0.″6 radius corresponding to the 1σ *Chandra* position uncertainty. Radio images use only data from April 2002, to provide the highest resolution. (a) The 3.6 cm image was made with uniform weighting (rms $\sim 27\mu$Jy beam^{-1}) and has a restoring beam of $0.''63 \times 0.''15$; contour levels are -0.10, 0.10, 0.15, 0.20, 0.40, 0.60, 0.90, 1.20, 2.00, and 3.500 mJy beam^{-1}. (b) The 2.0 cm image was made with 12 minutes of data and uses natural weighting (rms $\sim 85\mu$Jy beam^{-1}); contour levels are -0.25, 0.25, 0.40, 0.70, 1.00, 1.50, 2.50 mJy beam^{-1}. (c) The 1.5-10keV image was made from 28ks of Chandra data, retrieved from the *Chandra* public archive; contours are at 6, 8, 10, 12, 15, 18, 24, 30, 45, 60, 75 counts.

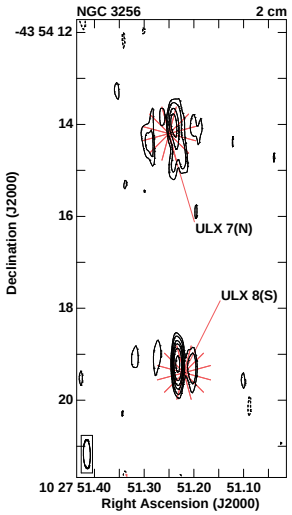

Fig. 2.— Continued

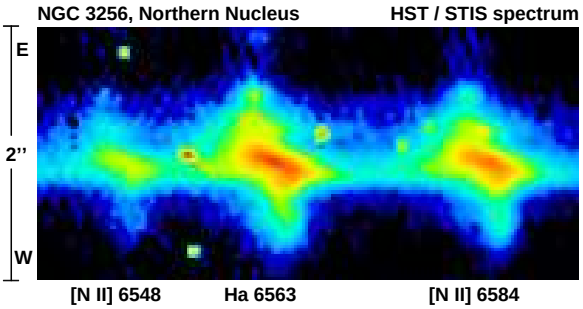

Fig. 3.— *HST* long-slit spectrum of the northern nucleus of NGC 3256, showing broad Hα and [N II]$\lambda\lambda$6548,6584Å emission lines. The emission lines indicate strong rotation around the nucleus, with a peak velocity shear of $\sim$300km sec^{-1} over a projected distance of $\sim$40pc. The $52\farcs0 \times 0\farcs2$ slit was oriented at a position angle of 91°, and two 340sec exposures were offset slightly along the slit. These and matching shorter wavelength spectra also show broadened lines from [S II]$\lambda\lambda$6717,6731Å and Hβ. (There are six blemishes in this subimage due to cosmic rays: one at the [N II]λ6548Å line ($0\farcs9$ above continuum), two between [N II]λ6548Å and Hα (one above, one below), one just longward of Hα and two just shortward of [N II]λ6584Å (all above the continuum).)

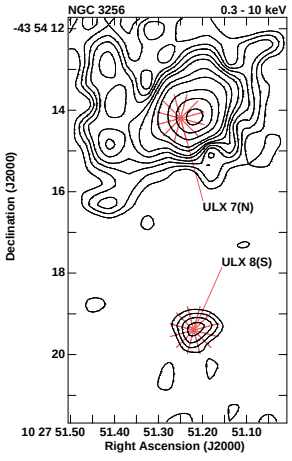

Fig. 2.— Continued